

Part II: Experimental Work and Applications

Chapter 6

Experimental Validation of the Theory

Much of the very early work in coupled oscillators for phased-array applications involved both theory and experiment. Probably the earliest was the work of Karl Stephan in which he studied a linear array of coupled oscillators for beam-steering of a linear array of radiating elements [1]. In his concept, the phasing was controlled by injection locking the end oscillators to signals whose relative phase was controlled with a phase shifter. While still earlier work was published, Stephan points out that it did not involve mutual injection locking, the defining feature of the concepts treated in this book.

6.1 Linear-Array Experiments

Stephan's pioneering experiment in 1986 involved three very high frequency (VHF) transistor Colpitts oscillators coupled together by a network of lumped elements. The end oscillators were also injected with external signals derived from a master oscillator signal that was split into two signals, one of which was phase shifted relative to the other by a variable length transmission line (coaxial line stretcher). Stephan measured the oscillator phases with varying amounts of phase shift of the injection signals and verified that the behavior conformed qualitatively to the theory. However, he noted several issues that have persisted throughout the ensuing development of this technology. He noted that manufacturing variation among the oscillators resulting in variation in their free-

running frequencies causes nonuniformity in the array behavior and indicated an appreciation of the fact that in his VHF oscillators this can be compensated for with tuning, but that in a monolithic microwave integrated circuit (MMIC) such adjustment would be more difficult. He did some statistical studies of this issue, and such studies were more recently extended by Wang and Pearson [50]. Their approach to mitigating this problem was to design the oscillator to minimize the phase slope of the open-loop gain. The impact of free-running frequency variation on beam pointing was studied by Shen and Pearson [51]. In his early work Stephan also discussed high-frequency application in spatial power combining and beam-steering, pointing out that there is potential for graceful degradation in the event of oscillator failure. Interestingly, he used a gradual phase shift of the injection signals (as discussed in Section 3.4 above) rather than a step-phase shift in time. The next year, Stephan and Young published theoretical and experimental results concerning two mutually injection-locked oscillators where the coupling was provided by the free-space mutual coupling between the radiating elements excited by them. [3] The coupling was represented by a two-by-two admittance matrix, and the stability of the two modes, even and odd, for the system was treated. The radiation patterns as a function of coupling phase; that is, element separation, showed behavior consistent with the analysis.

Three years later, Robert York, then a student working under Professor Richard Compton at Cornell University, published the results of a study of power combining in mutually injection locked Gunn diode oscillators arranged in a four-by-four planar array with Cartesian coupling [4]. Beam steering, however, was not considered; probably at least partly motivated by the publication by James Mink, the emphasis was on power combining [8]. Shortly thereafter, York and Compton published a description of mode locking in arrays of coupled oscillators [5]. They also described excitation of a linear array of radiating elements with a set of mode-locked oscillators [6]. The experiment described involved three Gunn-diode oscillators at 11 GHz. Although beam-steering is discussed, the concept is not the usual phased-array approach to scanning. Rather, mode locking is used to obtain a train of pulses that continuously scan at a rate determined by the spacing of the spectral lines of the periodic pulse train. (See Section 6.5)

Later in 1992, Hall and Haskins described a two-oscillator element designed for implementation of Stephan's external locking scheme for beam-steering [52]. A four-element array of 2.28-GHz elements was constructed, and beam-steering to 40 deg from normal was demonstrated.

A turning point was reached in 1993 with the publications by York and his student Peter Liao, in a special issue of the *IEEE Transactions on Microwave*

Theory and Techniques edited by Mink and Rutledge on Quasi-Optical Techniques [53] [28]. The reported analysis and experiment marked the first application of mutually injection-locked oscillator arrays to beam-steering via detuning of the end oscillators and no external injection. Liao and York constructed a four-element linear array of 10-GHz field effect transistor (FET) oscillators driving radiating elements that also served as resonators for the oscillators. Inter-oscillator coupling was due to mutual coupling among these radiating elements and fell in the weak-coupling regime. Beam steering to 15 deg from normal was achieved, and the theoretical and experimental results agreed quite well.

In the same special issue discussed above, Nogi, et al. described analysis and experimental work with strongly coupled Gunn-diode oscillators at 12.45 GHz [17]. They showed analytically that the array could oscillate in a number of modes, only one of which had constant amplitude across the array as might be desirable in excitation of a phased-array antenna, and they suggested that a resistor at the center of each coupling line would favor this desired mode and suppress the others.

By 1994 the use of coupled oscillators to excite phased array antenna elements and steer the radiated beam had become a vital and growing area of research. Liao and York reported a six-element microstrip patch array at 4 GHz that could steer to 40 deg from normal [54]. This array did not depend on mutual coupling between the radiating elements for coupling. Rather, the coupling was achieved with transmission lines connected between neighboring patches. This was the first attempt at decoupling the oscillator array design from the radiating aperture design. Later the same year a similar five-element array was reported that steered from -30 to $+40$ deg from normal. The associated theoretical treatment was based on a general admittance matrix description of the coupling network [33]. In 1997, a similar coupling scheme was used by Ispir, et al. in demonstrating the first planar array steered via detuning of the edge oscillators [55]. The array was three elements by three elements and coupled in a Cartesian topology. Thus, all but one element are edge elements. The beam was scanned 10 deg in the E plane and 15 deg in the H plane. Experiments with and without half-length coupling lines at the ends of a linear array were conducted, and it was found that the scan range was larger with the added lines. Kagawa, et al. demonstrated beam-steering in arrays with two and three circularly polarized elements [56], and Ispir, et al. experimented with unidirectional coupling in a three element array [55]. They showed that extended inter-oscillator phase range could be had by switching between two different values of coupling phase while steering via detuning the free running frequencies [57]. A very nice compendium of the work prior to 1997 is provided by Lynch, et al. in the book by York and Popovic on power combining [58].

During the development of these oscillator arrays, there was a concern about the phase noise of the oscillators and the possibility that arrays of many oscillators of wide-locking range might have prohibitively large phase noise. As a result an injection signal from an external stable oscillator might be needed. This was investigated by Chang, et al. [59]. Using a five-element array at 8.5 GHz, they demonstrated reduction of the array phase noise to the level of the injection source phase noise near the carrier frequency.

In August of 2000, Pogorzelski, et al. reported a seven-element linear array feeding a radiating aperture consisting of seven microstrip patches at 2.5 GHz [60]. Commercial MMIC voltage-controlled oscillators [Pacific Monolithics PM 2503] were used. This array is shown in Fig. 6-1. The coupling lines are visible on the circuit board as are the shorting bars used to adjust the coupling phase.

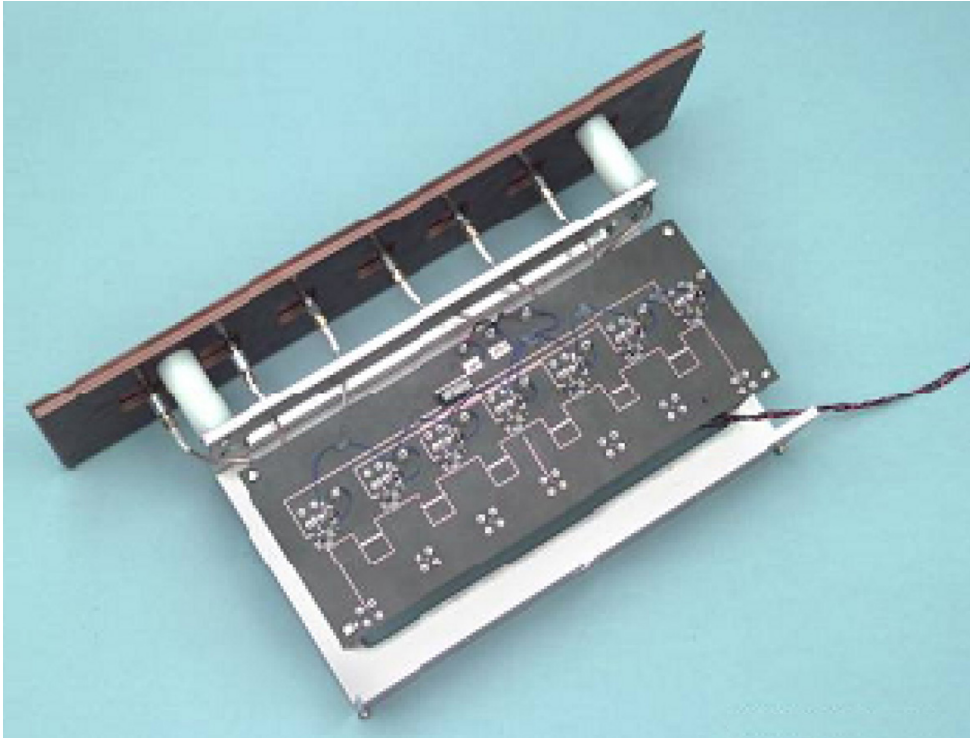


Fig. 6-1. Seven-element linear array. (Reprinted from [60] with permission, ©2001 IEEE.)

Initially, tuning of the oscillators was accomplished by using a network analyzer to measure the phase difference between adjacent oscillators, one pair at a time, and adjusting the free running frequencies to achieve the desired phase distribution. This process was impractically time consuming so a multichannel phase comparator system was devised that measured the phase differences between all adjacent oscillators simultaneously. This system consisted of a set of quadrature hybrid couplers and mixers arranged as shown in Fig. 6-2. The oscillator output signals from neighboring oscillators were mixed, and the lower hybrid frequency was at zero frequency. This DC output voltage was taken to be a measure of the relative phase of the oscillator signals. The hybrid couplers introduced a 90-deg phase shift in one of the signals so that zero output voltage from the mixer corresponded to zero relative phase. The output voltages from the mixers were then integrated from the center outward using a virtual instrument implemented in LabView™ to produce a graphical representation of the aperture phase distribution as shown in Fig. 6-3. The mixer outputs are shown in the bar graph, and the phase distribution is shown in the line graph below.

This seven-element array was evaluated on an antenna measurement range, and the patterns compared with predictions for both unscanned and scanned beams. The results are shown in Fig. 6-4.

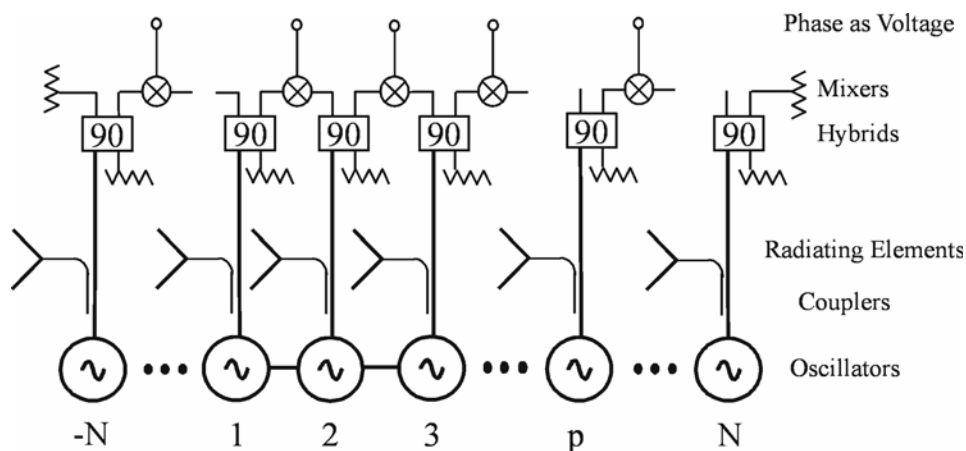


Fig. 6-2. Phase measurement system. (Reprinted from [61] with permission, ©2000 IEEE.)

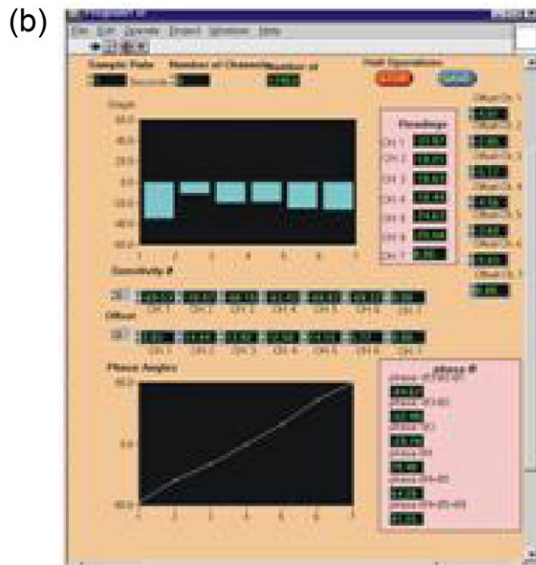
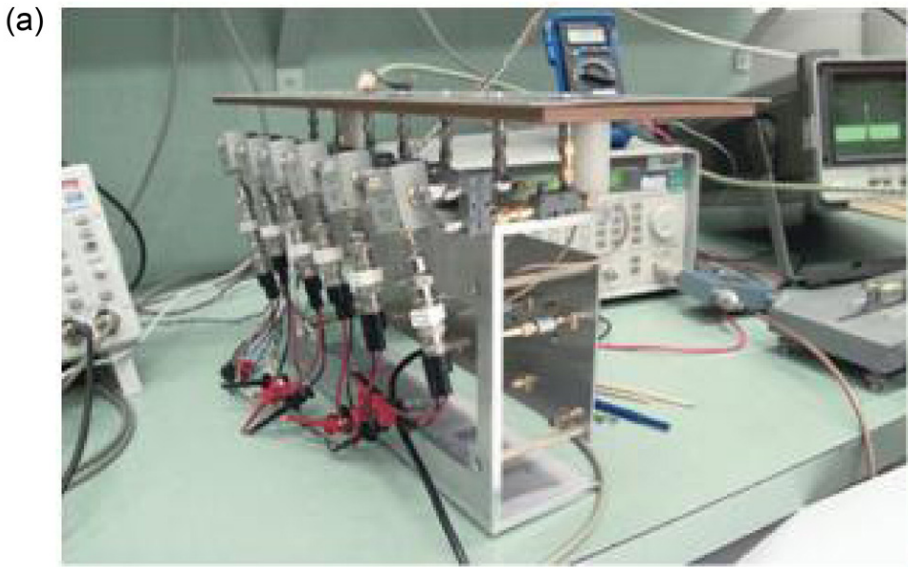


Fig. 6-3. Virtual instrument showing (a) multichannel phase comparator connected to the seven-element array and (b) a screen capture of the virtual instrument computer display. (Reprinted from [62] with permission, ©2006 IEEE.)

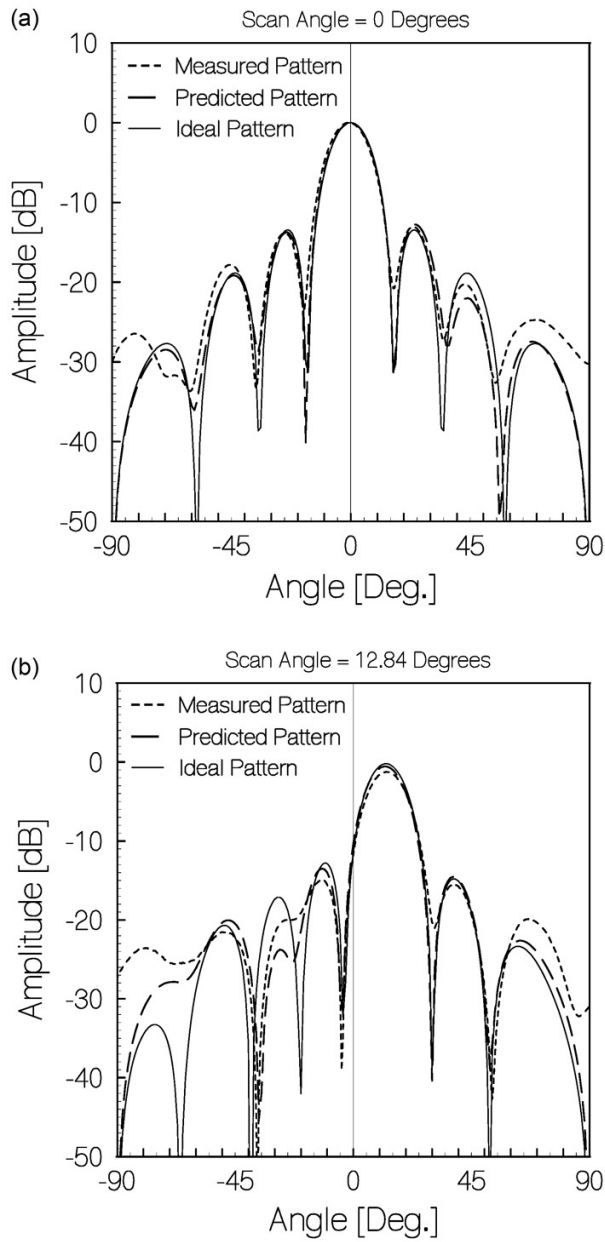


Fig. 6-4. Unscanned and scanned beams from the seven-element array with amplitude plotted against angle for unscanned and scanned beams at (a) 0-deg scan angle and (b) 12.84-deg scan angle. (Reprinted from [60] with permission, ©2000 IEEE.)

In Section 3.1 we obtained the transient behavior of the oscillator phases under step detuning of one oscillator. The seven-element array described above was also used to experimentally confirm that result [63]. One oscillator was repeatedly detuned by applying a tuning signal from a pulse generator, and the repeated transient behavior was recorded digitally using a multi-channel oscilloscope. The results, both experimental and theoretical, for detuning one end oscillator are shown in Fig. 6-5. Figure 6-6 shows a similar comparison when one interior oscillator is step detuned.

Recently, preliminary results on coupled oscillator arrays implemented using substrate integrated waveguide technology (SIW) have been reported. Substrate integrated waveguide (SIW) technology allows for compact, low cost, light weight, and high performance implementation of microwave active and passive circuits, including active antennas and coupled oscillator arrays. SIW structures were initially proposed in the mid-1990s [64]. SIWs are waveguide-like structures fabricated by using two periodic rows of metallic vias or slots connecting the top and bottom ground planes of a dielectric substrate. An SIW cavity backed coupled oscillator antenna array, shown in Fig. 6-7 was proposed by Giuppi et al. [65].

SIW structures share advantages of both microstrip and waveguide technology [66]. Similarly to planar structures, SIWs are compact, light weight, and cost effective due to the fact that they can be easily fabricated on single substrates using conventional fabrication techniques such as the ones used for their planar counterparts. Similarly to waveguide structures they exhibit increased shielding, low loss, high quality factor, and high power-handling capability. Finally, they allow for high integration by implementing multilayer architectures. SIW technology allows for compact, low cost implementation of coupled-oscillator arrays, suitable for large array configurations.

Giuppi et al. demonstrated a single substrate implementation of a cavity-backed coupled-oscillator antenna array [65]. A two-element slot-array prototype that was implemented is shown in Fig. 6-7. Cavity-backed antennas have received interest due to attractive properties such as isolation, reduction of backward radiation, and surface-wave suppression [67].

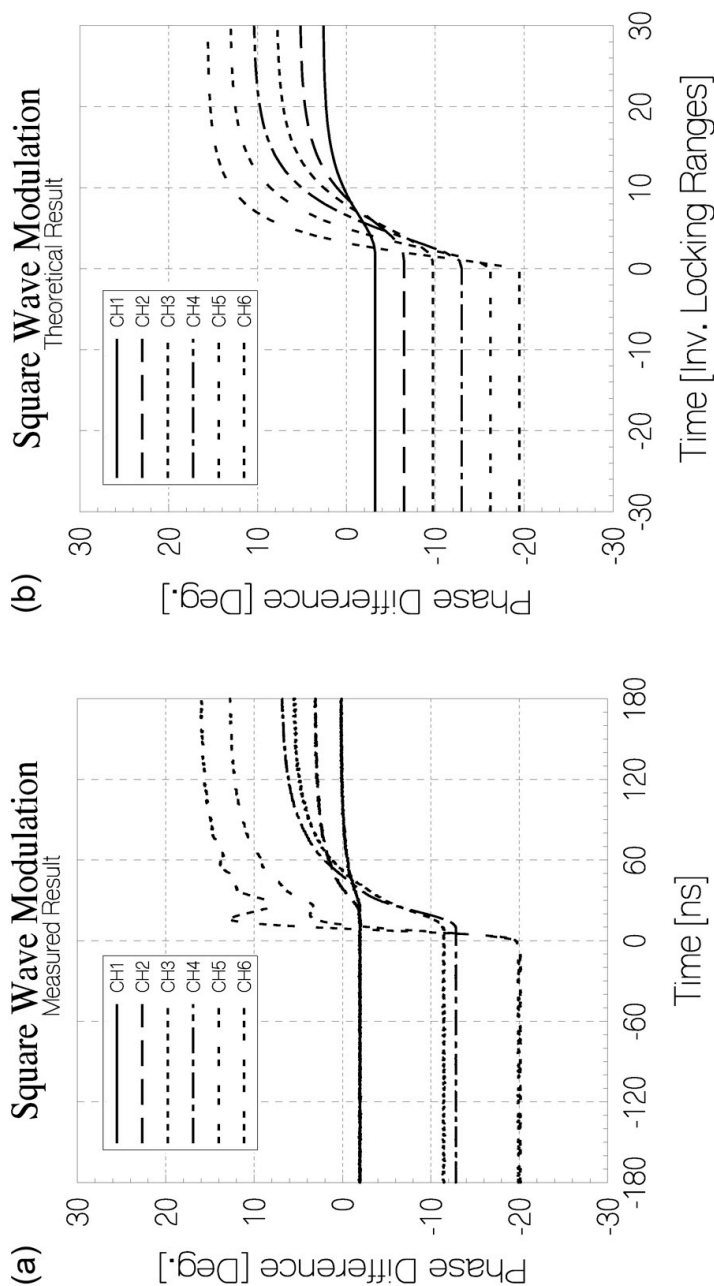


Fig. 6-5. E-plane transient response of the seven-oscillator array with one end oscillator step detuned for (a) experimental results and (b) theoretical results. (Reprinted from [63] with permission, ©2002 IEEE.)

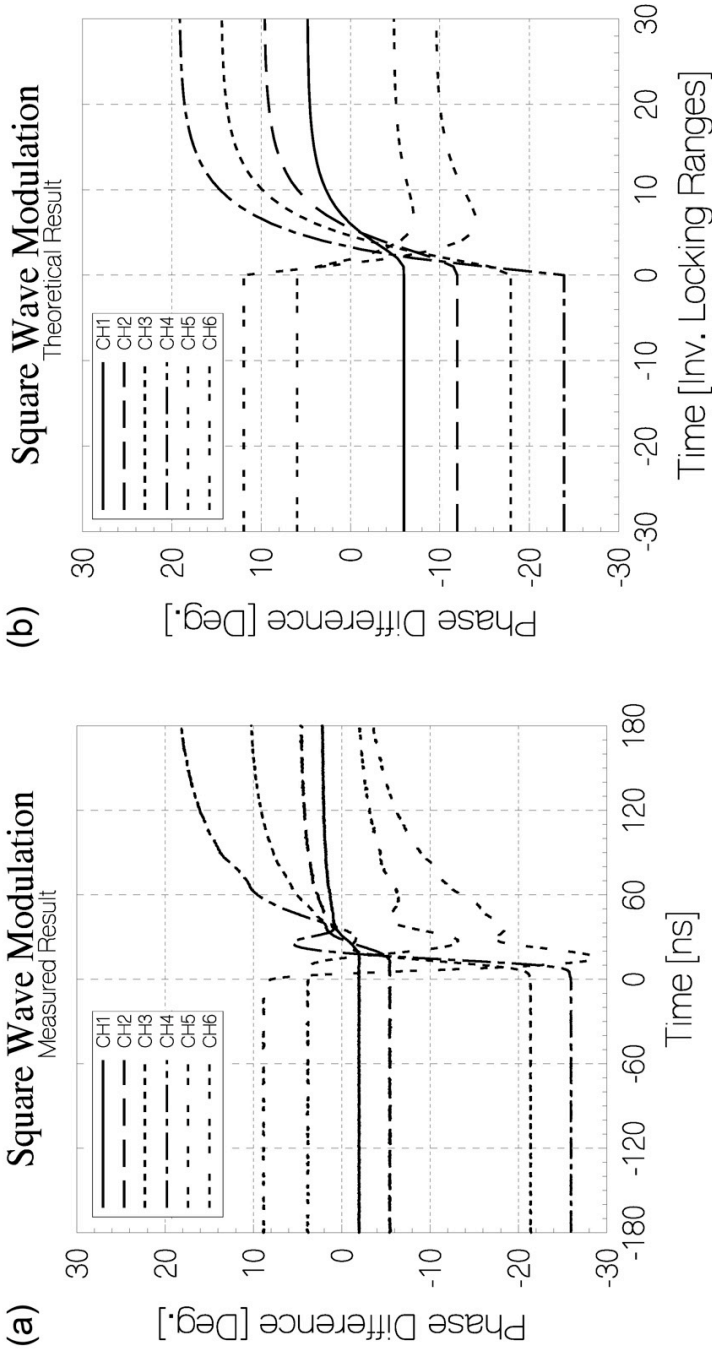


Fig. 6-6. H-plane transient response of the seven oscillator array with one interior oscillator step detuned for (a) experimental results and (b) theoretical results. (Reprinted from [63] with permission, ©2002 IEEE.)

In the work of Ref. [65], SIW technology was used to fabricate cavity-backed slot-antenna oscillators and additionally control the coupling among the oscillator elements. The effect of the coupling aperture size A on the coupling strength is shown in Fig. 6-8. It was found that a double aperture symmetrically placed around the middle of the cavity wall, such as the one used in Fig. 6-7, leads to a smoother variation of the coupling factor as a function of the aperture size, compared to a single aperture at the center of the cavity wall, and therefore is less sensitive to fabrication tolerances.

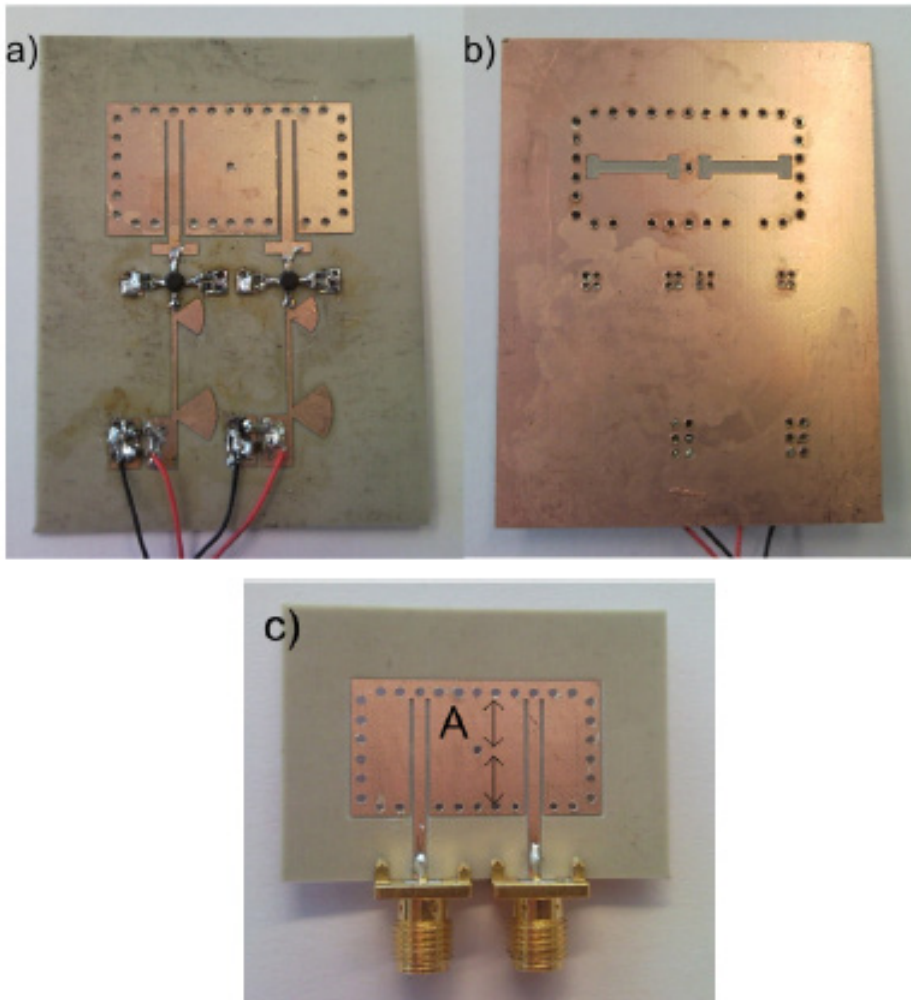


Fig. 6-7. Single-substrate two-element cavity backed coupled oscillator antenna array in SIW technology, a) top (active circuit) side, b) bottom (antenna) side, c) passive antenna array. Reprinted with permission from [65]; copyright EurAAP 2010; used with permission.

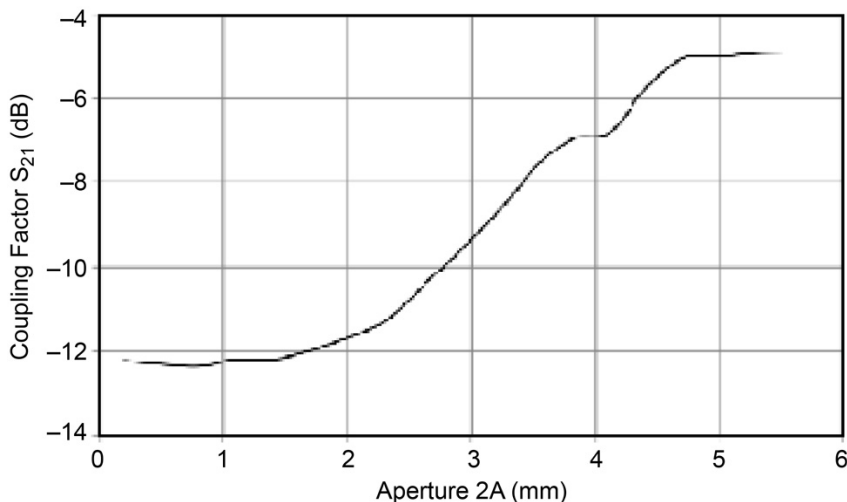


Fig. 6-8. Coupling factor versus the aperture size between the cavities of Fig. 6-7. Reprinted from [65]; copyright EurAAP 2010; used with permission.

Finally, it is possible to control the oscillation frequency of the active oscillator antenna by varying the resonance frequency of the cavity. This is achieved by removing one of the vias from the cavity wall and placing a varactor diode in the cavity providing a capacitance between the top cavity conductor and the bottom ground conductor. Using this topology a frequency tuning of approximately 2 percent was demonstrated by Giuppi et al. in [68] (Fig. 6-9).

6.2 Planar Array Experiments

A planar three-by-three oscillator array was reported by Pogorzelski in 2000 [61]. Recall that Ispir also reported a three-by-three array in 1997 using coaxial transmission line coupling between the radiating elements [55]. However, the 2000 array by Pogorzelski had no radiating aperture. Its purpose was to demonstrate phase control by perimeter detuning via a phase diagnostic system similar to that developed for the seven-element linear array. Basically, the linear array diagnostic system was “woven” through the planar array one row at a time, and the computer-based virtual instrument was reprogrammed to display the computed phase values in a planar representation. This array is shown in Fig. 6-10. The precision potentiometers control the tuning bias of each oscillator.

The phase distributions over the array with various oscillator detuning distributions are shown in Fig. 6-11.

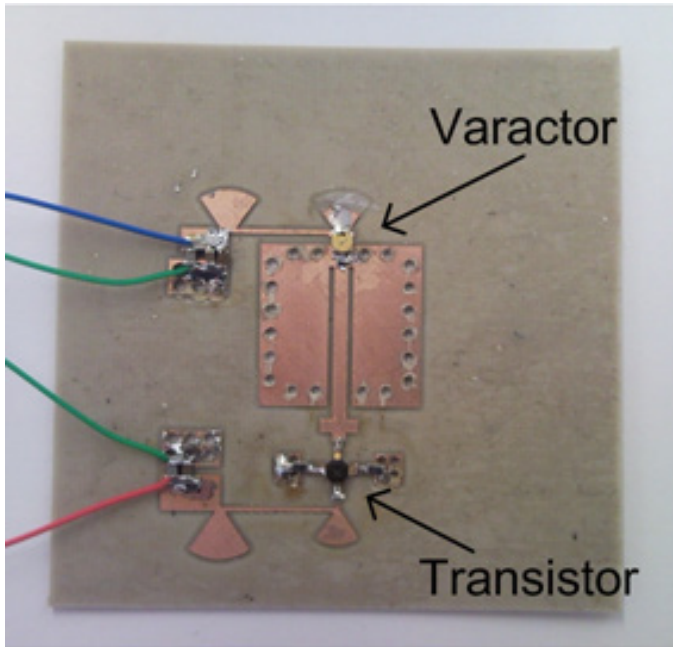


Fig. 6-9. SIW cavity-backed active-oscillator slot antenna with frequency tuning capability. (Reprinted with permission from [68], IET.)

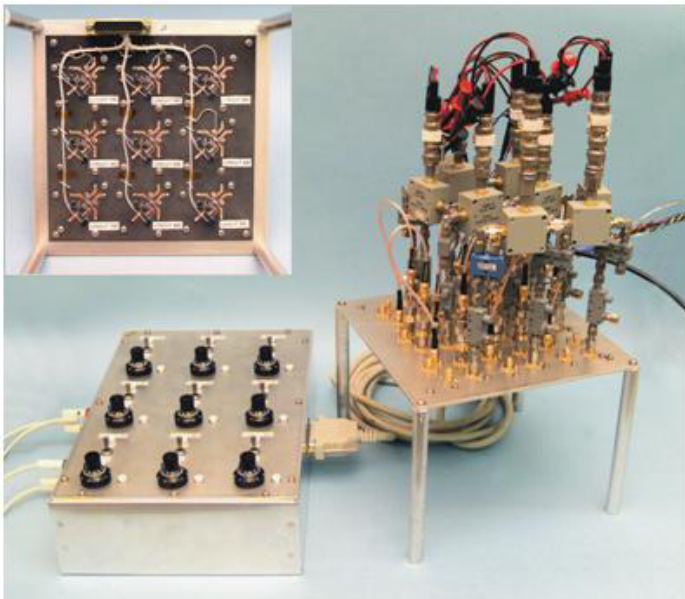


Fig. 6-10. Nine-element planar oscillator array. (Reprinted from [62] with permission, ©2006 IEEE.)

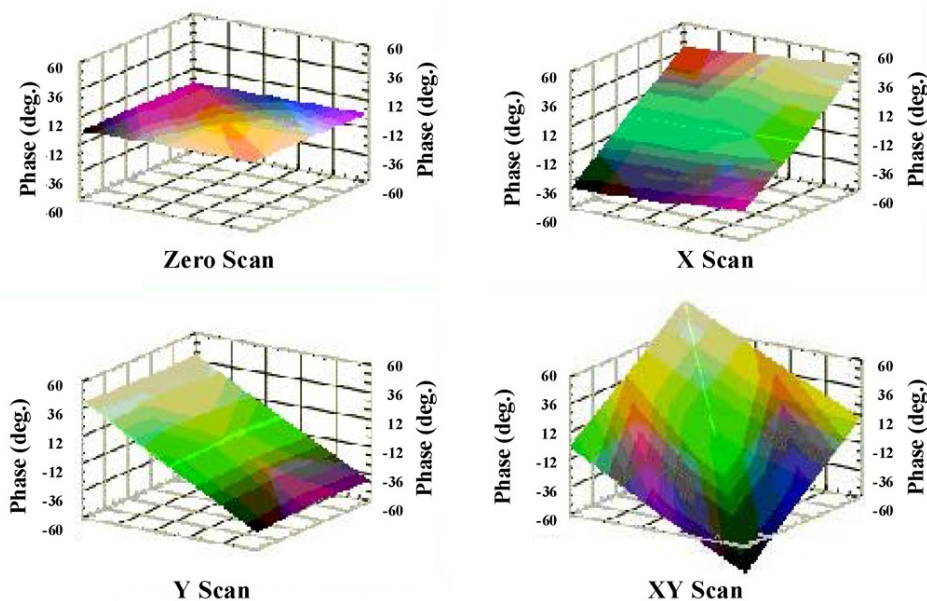


Fig. 6-11. Screen captures of phase distributions for beam-steering in a planar array. (Note: The tonal scale redundantly duplicates the phase vertical scale). (Reprinted from [61] with permission, ©2000, IEEE.)

As discussed earlier, the maximum phase difference between adjacent oscillators is 90 deg, at which value the oscillators lose lock. This limits the attainable beam-steering angle from normal. However, as described by York and Itoh, this range may be extended by frequency multiplication, which also multiplies the phase excursion [40]. To demonstrate this technique, frequency triplers were added to the above nine-element array, and the resulting 8.4-GHz output was used to drive a nine-element microstrip patch array. The aperture phase was inferred by tripling the outputs of the mixers in the slightly more sophisticated diagnostic system shown in Fig. 6-12, and the resulting far-zone radiation patterns were measured on an antenna range. Note that, unlike its predecessor, this diagnostic system uses attenuators to equalize the input amplitudes at the mixers. The measurement set-up is shown in Fig. 6-13 wherein the coaxial line stretchers equalize the phases of the transmission lines to the radiating elements. The resulting measurements are shown in Fig. 6-14 where the “X’s” label a pattern that corresponds to steering 90 degrees from normal which is not achievable without frequency multiplication. Note that this pattern is symmetric indicating that the main lobe points 90 deg to the left while the similar looking lobe on the right is a grating lobe. The element pattern is shown as the dashed curve and indicates why all of the patterns have a null 90 deg from normal. In 2005, Pogorzelski reported construction and demonstration of a five-by-five element planar array using using the same S-band MMIC oscillators used in the

earlier seven-element linear array and microstrip patch radiating elements [70]. This MMIC contained a buffer amplifier at its output, thus isolating the oscillators and patches and completely separating the coupled oscillator array design from the radiating aperture design. In this array, the oscillators were located on one side of a Duroid™ board, and the patches located on the other with a coaxial pin connecting each oscillator output to the corresponding patch. The phase-measurement system was mounted on a phenolic board for physical support and connected to the oscillators via stripline couplers obviating the need for direct physical connection and rendering the measurement system removable. The assembled array and phase measurement system is shown in Fig. 6-15. The Duroid™ circuit board is located between the aluminum plate and the phenolic board.

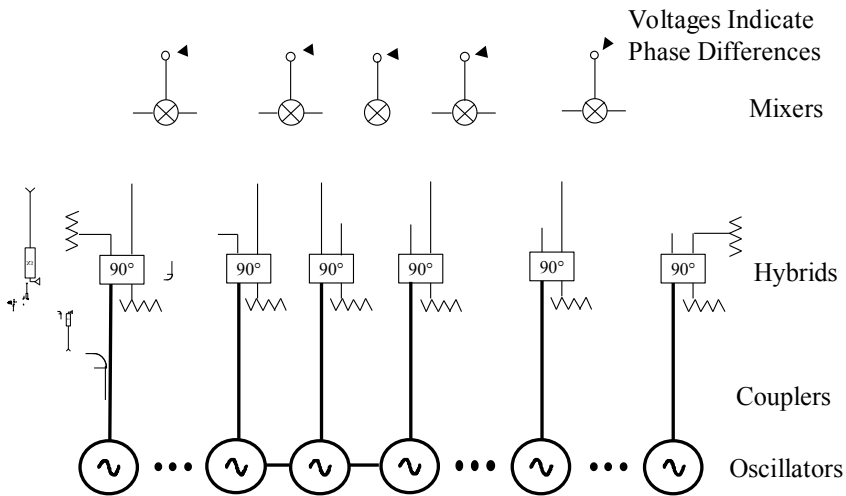


Fig. 6-12. Phase measurement system for the frequency-tripled array. (Reprinted from [69] with permission, ©2004 IEEE.)

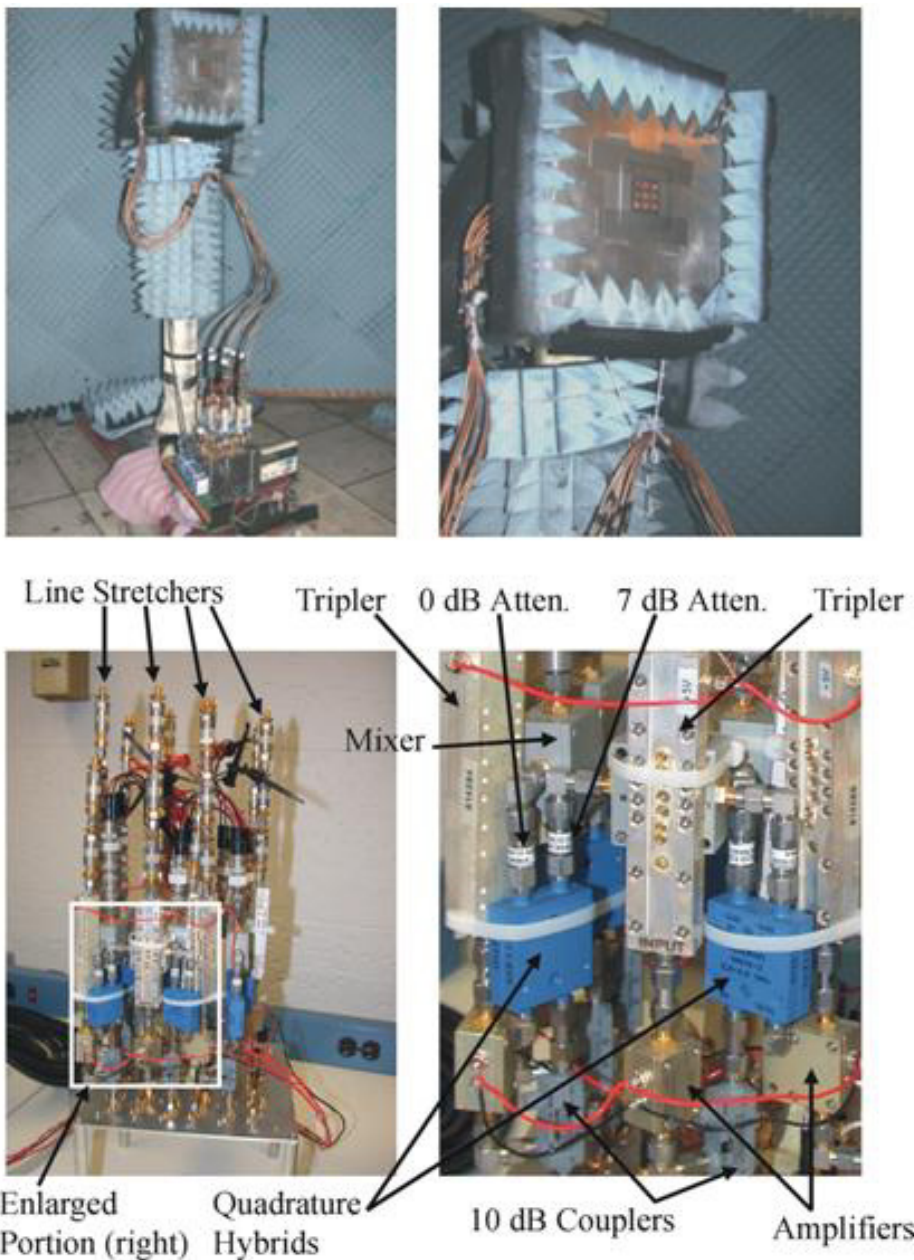


Fig. 6-13. Experimental set-up for evaluation of the nine-element frequency tripled planar array. The white box of the lower left picture is enlarged in the lower right picture. (Reprinted from [69] with permission, ©2004 IEEE.)

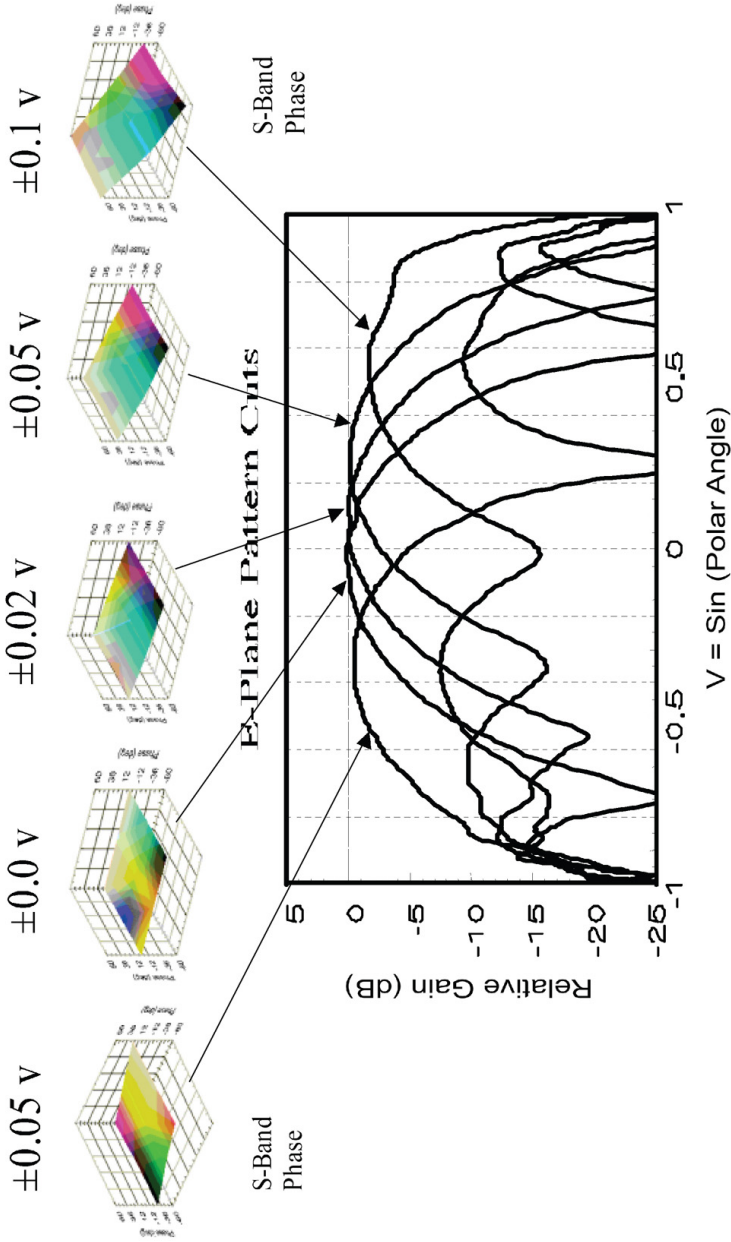


Fig. 6-14(a). Measured phase distributions and antenna patterns of the nine-element frequency tripled planar array showing E-plane pattern cuts. The vertical axis of the small phase surface plots ranges from -60 to $+60$ degrees of phase, and the total scale redundantly duplicates this same information. (Reprinted from [69] with permission, ©2004 IEEE.)

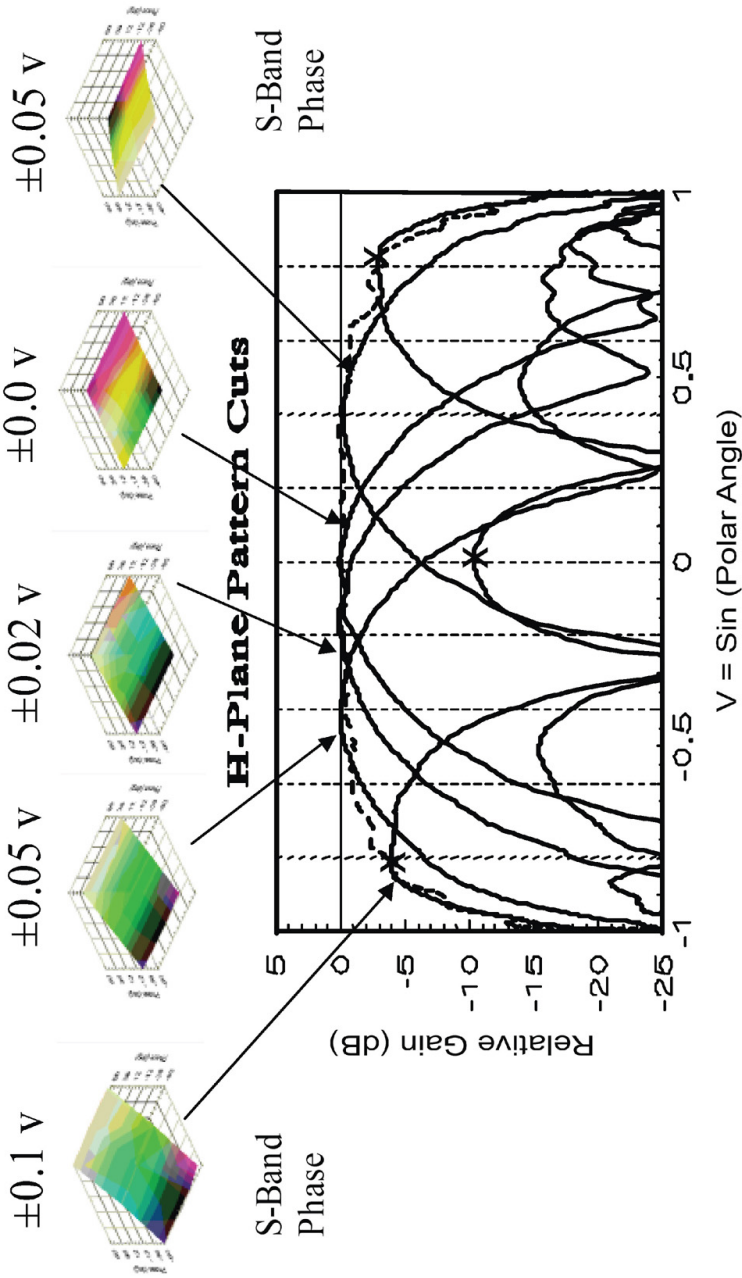


Fig. 6-14(b). Measured phase distributions and antenna patterns of the nine-element frequency tripled planar array showing H-plane pattern cuts. The vertical axis of the small phase surface plots ranges from -60 to $+60$ degrees of phase, and the tonal scale redundantly duplicates this same information. (Reprinted from [69] with permission, ©2004 IEEE.)

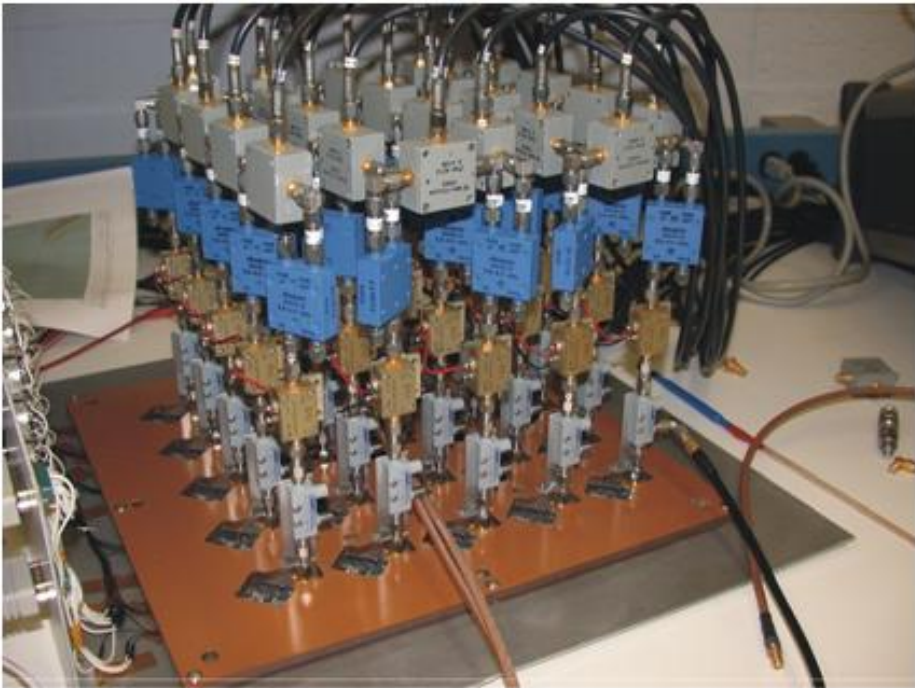


Fig. 6-15. Five-by-five S-band array and phase-measurement system. (Reprinted from [62] with permission, ©2006 IEEE.)

The Duroid™ board and aluminum plate attached to the measurement fixture are shown in Fig. 6-16. The array of potentiometers controls the power supplied to each oscillator and were used to approach an untapered aperture distribution for the array. Fig. 6-17 shows the assembled array on the measurement range and Fig. 6-18 shows an example measured result for aperture phase distribution and steered beam.

A similar five-by-five element array was reported by Heath, et al. [71] of the Georgia Tech Research Institute (GTRI) using a new phase comparator chip that rendered the phase measurement system much more compact. In fact it was integrated with the oscillator array shown in Fig. 6-19. The GTRI group used a LabView™-based display system very similar to that of Pogorzelski [70]. However, unlike Pogorzelski, GTRI also used a LabView™ user interface for tuning the oscillators. (See Fig. 6-20.) This GTRI array was similar to the three-by-three frequency tripled array discussed earlier in that the oscillators were connected to the radiating aperture via cables visible in Fig. 6-21 showing the near-field test set-up at GTRI. However, it did not use frequency multiplication as did the three-by-three array. Figure 6-22 displays an example near-field measurement transformed to the far-zone showing the beam steered to -20 deg.

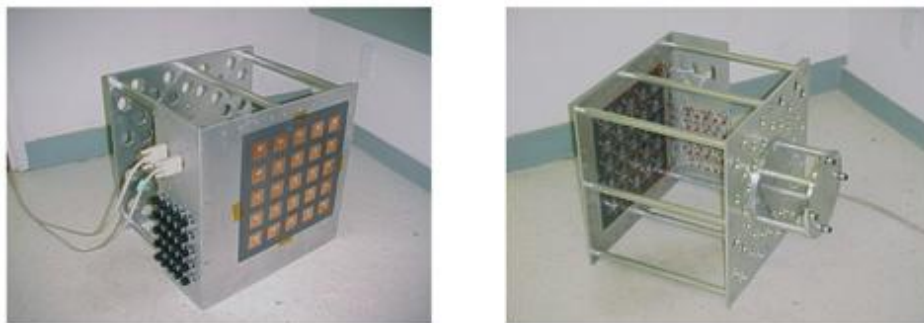


Fig. 6-16. Five-by five oscillator array and radiating aperture on measurement fixture. (Reprinted from [62] with permission, ©2006 IEEE.)

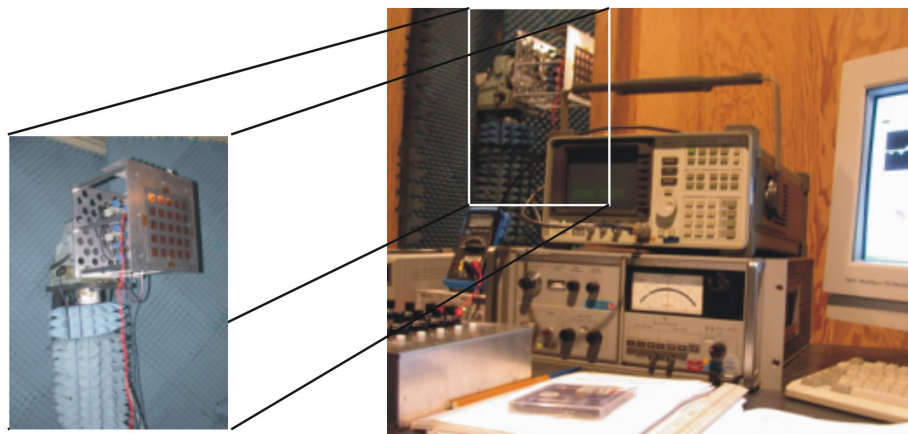


Fig. 6-17. Five-by-five array on the measurement range. (Reprinted from [62] with permission, ©2006 IEEE.)

The ability to electronically control the phase differences among the synchronized elements of a coupled oscillator array by varying the free-running (uncoupled) frequency of each element has been used by Yen and Chu in order to simultaneously scan and control the polarization of a linear antenna array [72].

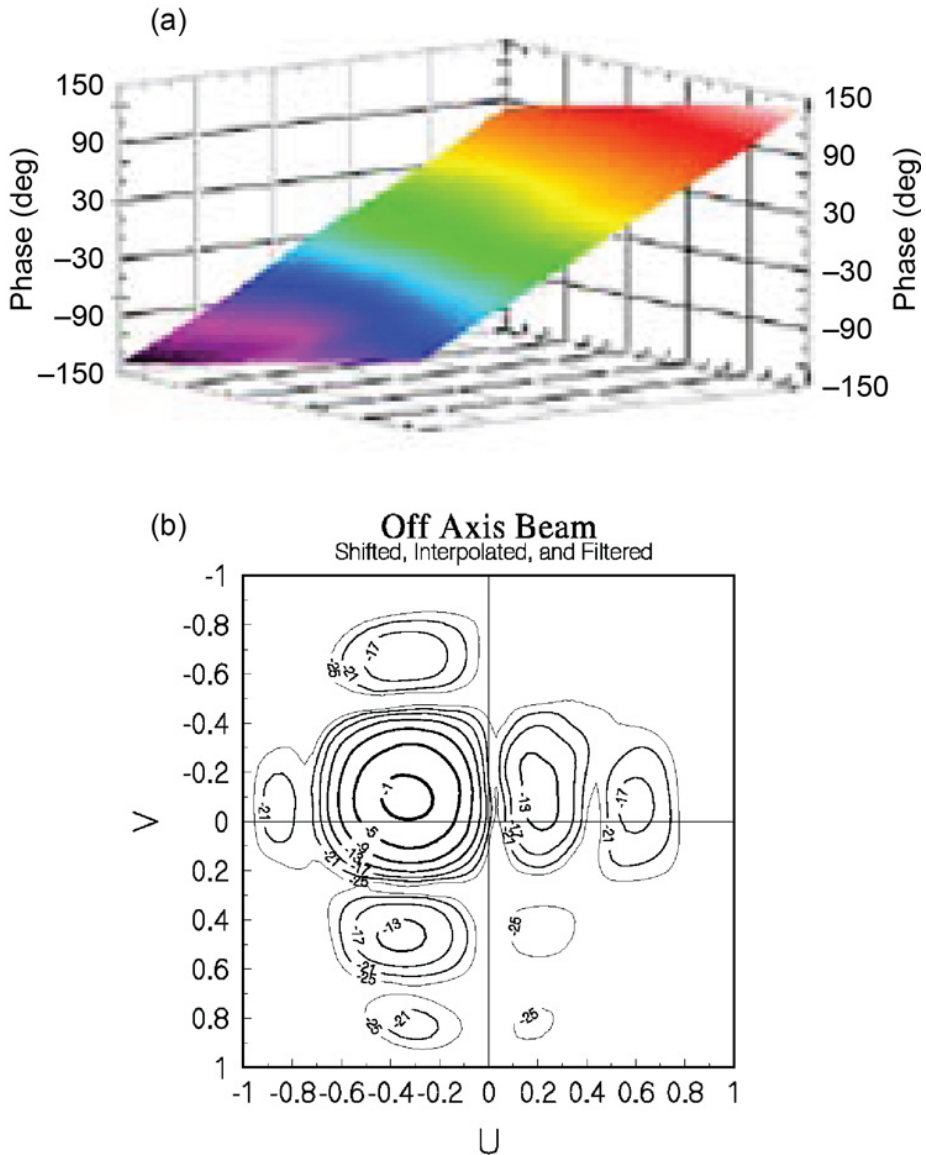


Fig. 6-18. Five-by-five array (a) Measured aperture phase and (b) Steered beam. (Note: The tonal scale redundantly duplicates the phase information in (a).) (Reprinted from [62] with permission, ©2006 IEEE.)

The block diagram of the proposed architecture is shown in Fig. 6-23. A linear dual linearly polarized patch antenna array of N elements is used as the radiating structure. A two-dimensional coupled oscillator array consisting of two rows of N oscillators is connected to the $2N$ antenna ports. The phase difference between the oscillator elements within each row is used to generate a

progressive phase distribution and steer the main beam of the array. The phase difference between the two rows controls the phase difference between the two orthogonal polarization states and therefore the polarization of the array. Frequency doublers are used at each oscillator output in order to produce a stable phase variation of up to 360 deg. A prototype consisting of a four element antenna array was successfully demonstrated [72] (Fig. 6-24).

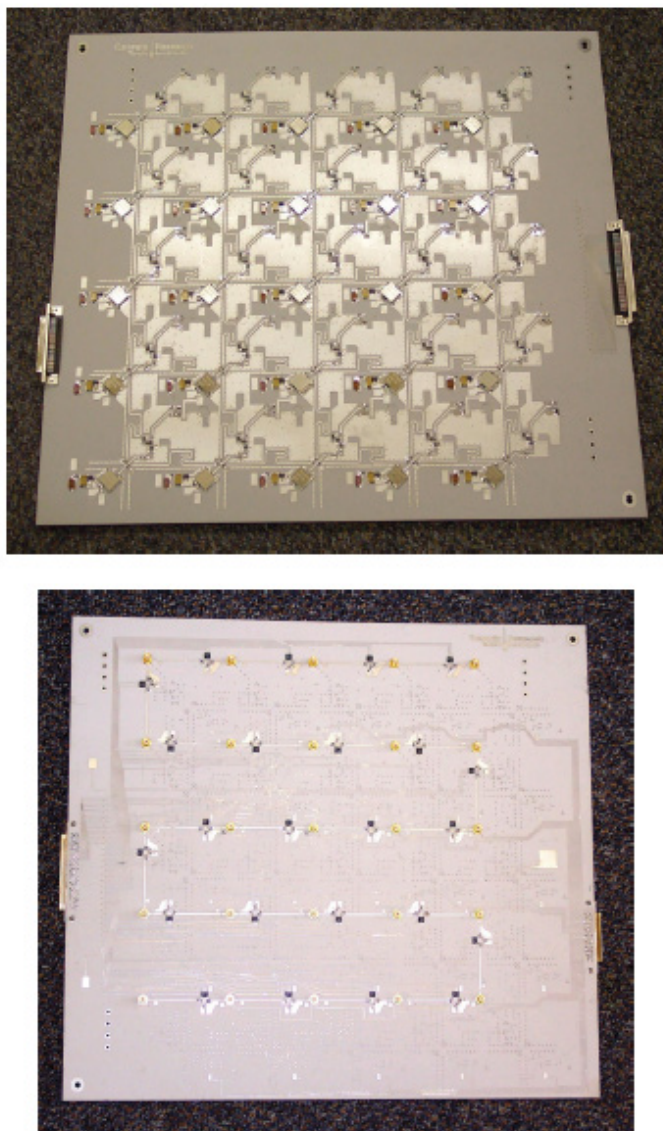


Fig. 6-19. Both sides of GTRI five-by-five oscillator array board. (Reprinted from [71] with permission, ©2005 IEEE.)

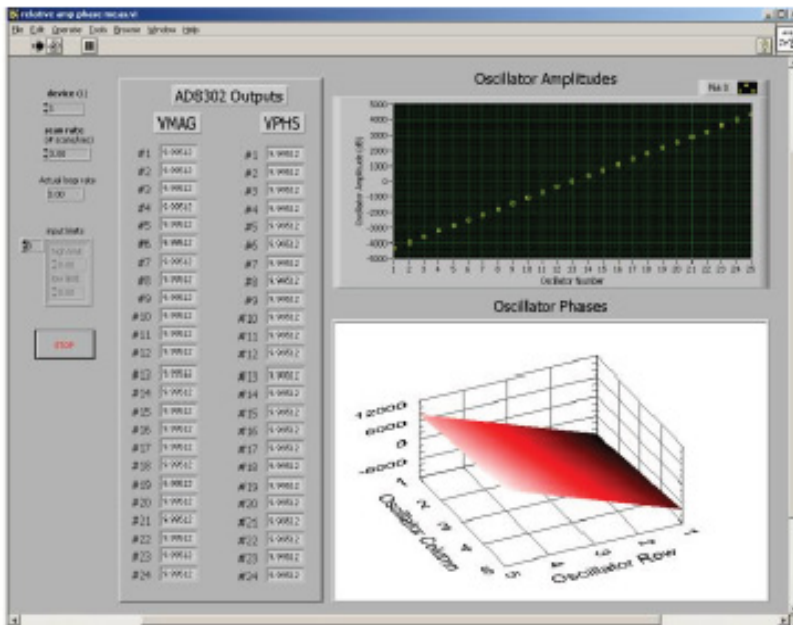
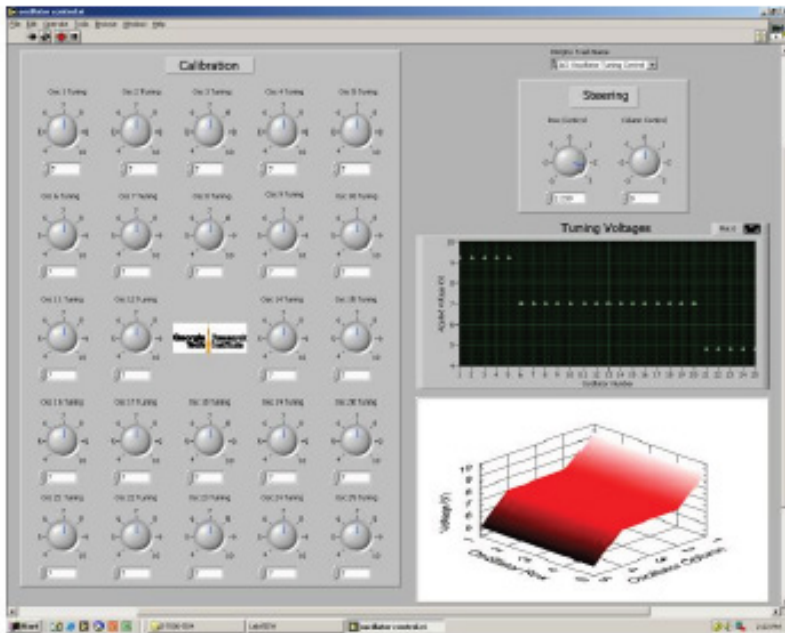


Fig. 6-20. Screen captures of the GTRI LabView virtual instrument for tuning (above) and phase measurement (below). (Reprinted from [71] with permission, ©2005 IEEE.)



Fig. 6-21. The GTRI test set-up for near-field measurement of the five-by-five array. (Reprinted from [71] with permission, ©2005 IEEE.)

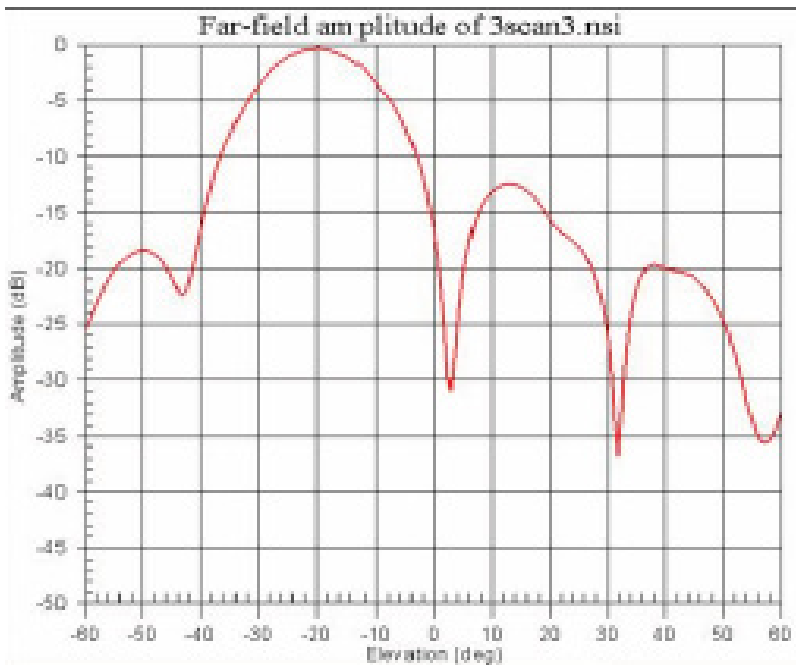


Fig. 6-22. Far zone steered beam of the GTRI five-by-five array. (Reprinted from [71] with permission, ©2005 IEEE.)

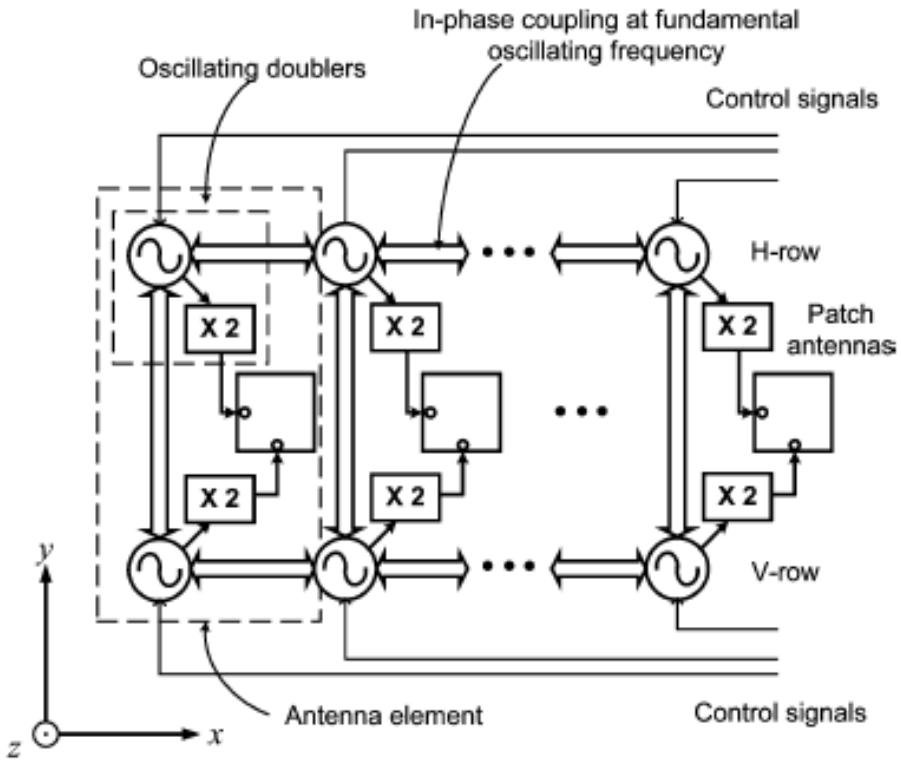


Fig. 6-23. Polarization agile, beam scanning coupled oscillator antenna array architecture. (Reprinted with permission from [72], ©2005 IEEE.)

6.3 Receive Array Experiments

As early as 1995 it was suggested by Cao and York that oscillator arrays could be used to steer the beam of a receiving antenna. [73]. The concept is illustrated in Fig. 6-25. Basically, the oscillators are used as local oscillators to down convert the signals received by each of the elements in antenna aperture. The phasing of the local oscillator signals may then be adjusted to cancel the phasing of the element signals due to the angle of arrival of the incident wave. Thus, the phasing of the oscillators as determined by detuning of the end oscillators may be said to steer the receive beam.

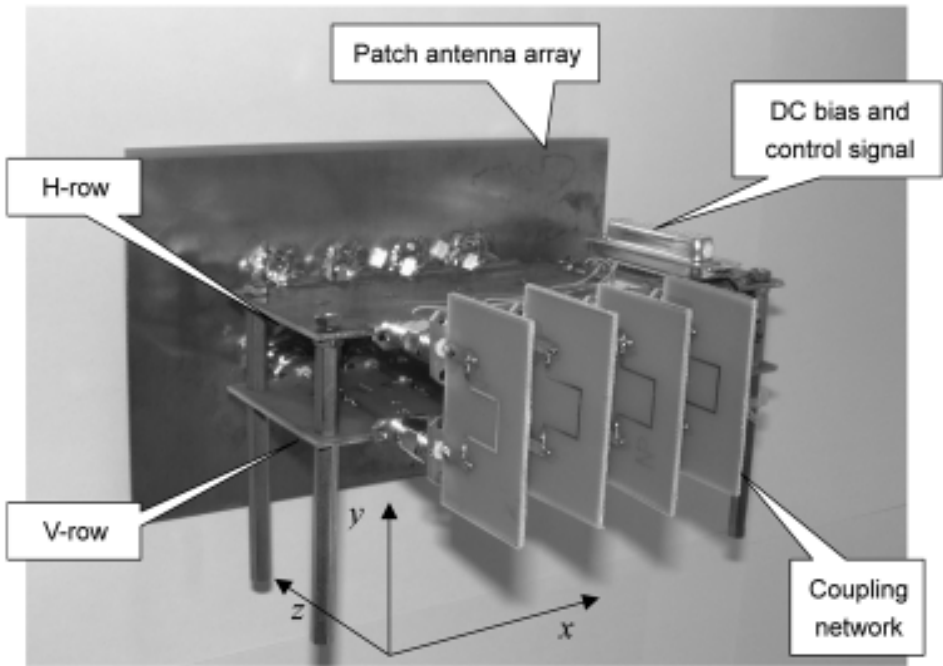


Fig. 6-24. Photo of a four-element prototype of the polarization agile, beam-scanning coupled oscillator antenna array (H-row = horizontal row and V-row = vertical row). (Reprinted with permission from [72], ©2005 IEEE.)

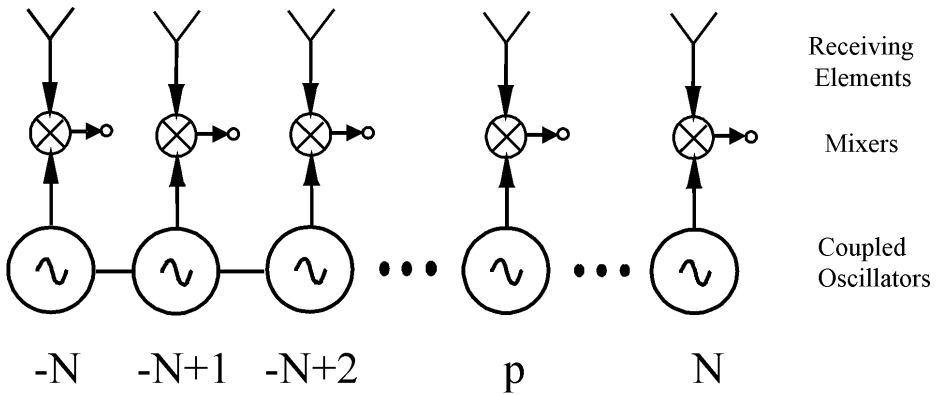


Fig. 6-25. Receive concept using coupled oscillators.

This concept was demonstrated experimentally by Pogorzelski and Chiha [74] using a 15-element array of L-band oscillators [Modco CM1398MST] coupled in a linear configuration. In the absence of a receiving aperture, the received signals were simulated using a 16-way power divider. These 1.95-GHz output signals from the power divider were, of course, in-phase. They were mixed with the 1.265-GHz outputs of the linear array oscillators producing intermediate frequency signals at 685 MHz. These intermediate frequency signals were then combined using another 16-way power divider in reverse. The testbed set-up is shown in Fig. 6-26 together with a closeup of one of the oscillator circuits. By using only every other oscillator in the array, the maximum phase difference between adjacent local oscillator signals was extended to 180 deg. Thus, only eight signals are combined. The combined output at 685 MHz is plotted versus beam-steering angle in Fig. 6-27. The solid line is the theoretically predicted result. The phase distributions across the array corresponding to points A and B are shown in Fig. 6-28.

This apparatus was also used to demonstrate a very interesting scheme patented by Kott for the reduction of sidelobes [75]. Kott proposed the placement of an additional element at each end of an array positioned and excited so as to provide an interferometer pattern with null spacing matching the null spacing of the sidelobes of the array. Then by properly combining the interferometer signal with the array signal, entire regions of sidelobes could be canceled. It turns out that the receive-array testbed described above provides just the proper phasing of the end elements to achieve this cancellation [76]. The concept is shown in Fig. 6-29. The attenuators at each end oscillator permit proper weighting of the interferometer signal relative to the receive array signal to achieve cancellation. Fig. 6-30 shows the output of the intermediate frequency combiner versus beam-steering angle for the center elements (solid), the interferometer pattern of the end elements (short dashes), and the coherent combination of the two (long dashes) showing that the left sidelobe has been removed while the right one has been enhanced. The beamforming capabilities of coupled oscillator arrays are studied in more detail in Chapter 9.

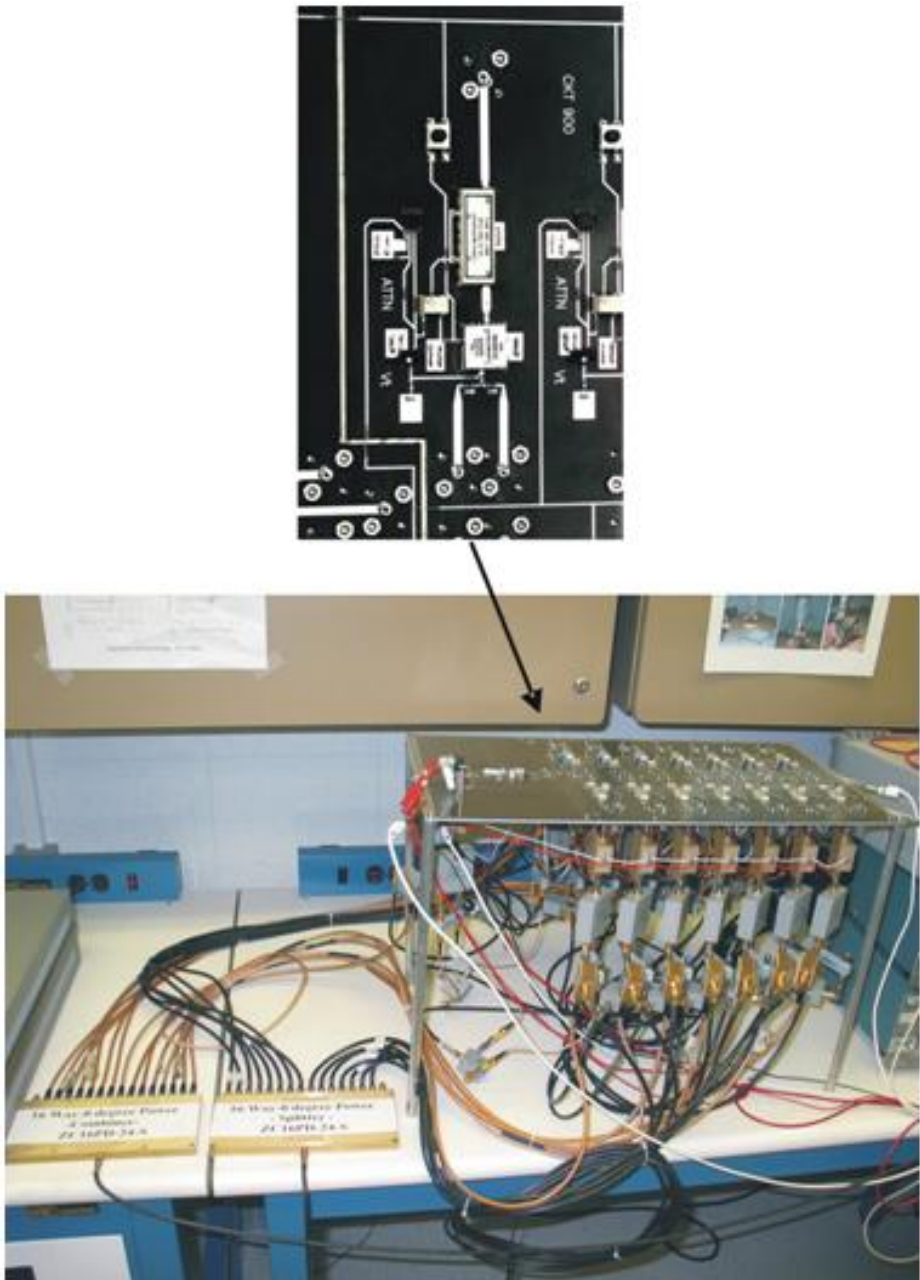


Fig. 6-26. L-band receive array test-bed with close-up of one oscillator. (Reprinted from [62] with permission, ©2006 IEEE.)

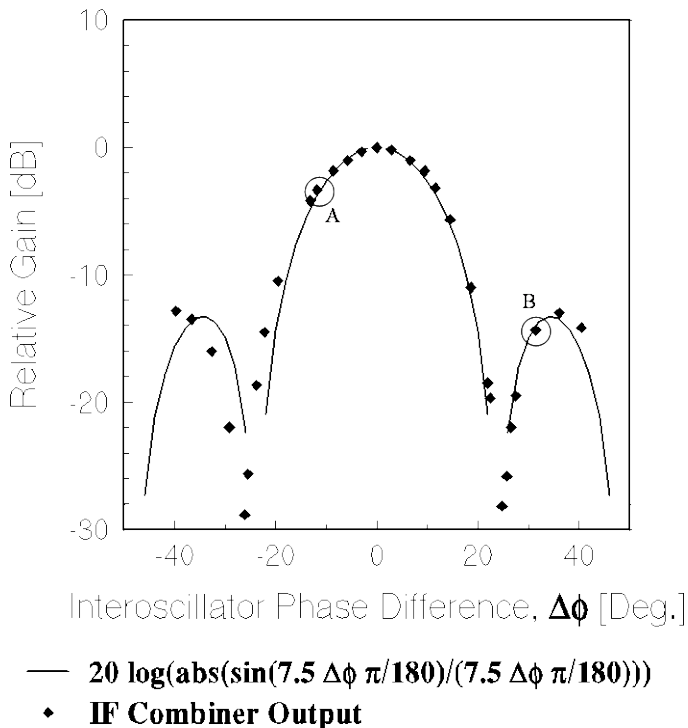


Fig. 6-27. Combined intermediate frequency signal versus receive beam-steering angle for the 15-oscillator L-band array. (Reprinted from [62] with permission, ©2006 IEEE.)

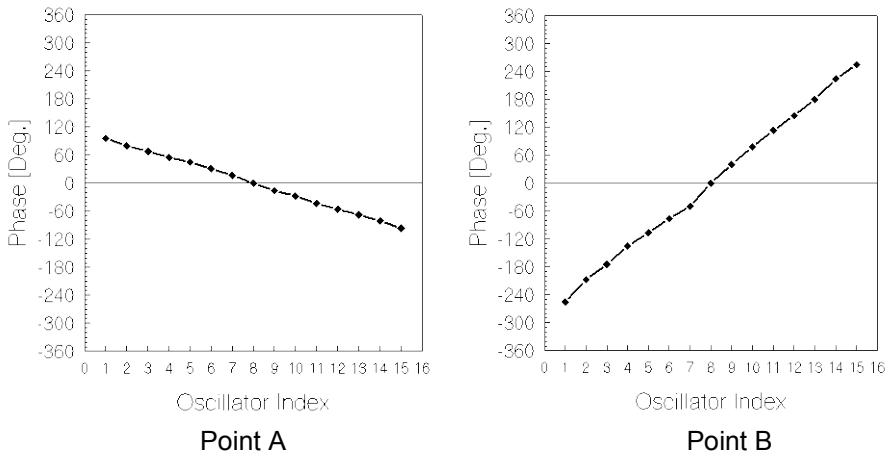


Fig. 6-28. Phase distributions corresponding to the two indicated points A and B in Fig. 6-27. (Reprinted from [62] with permission, ©2006 IEEE.)

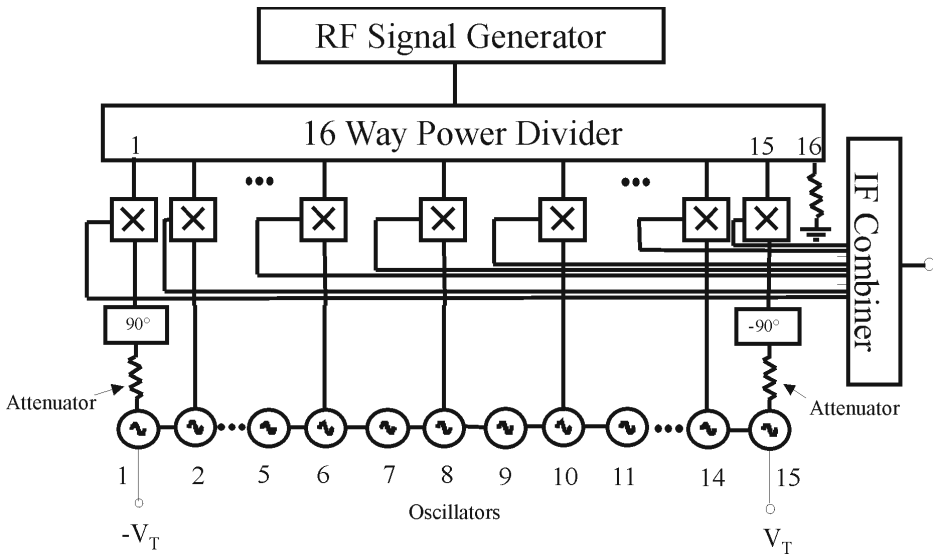


Fig. 6-29. Circuit arrangement to implement the Kott scheme using the fifteen element receive array testbed. (Reprinted from [62] with permission, ©2006 IEEE.)

Receive Patterns

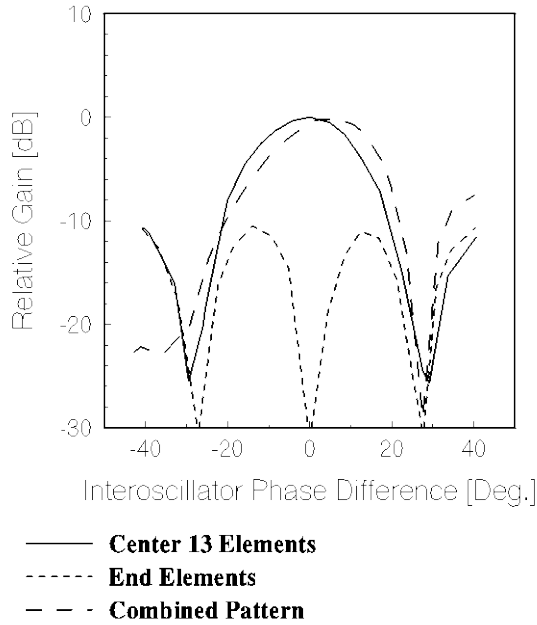


Fig. 6-30. Pattern plots showing cancellation of the left sidelobe. (Reprinted from [62] with permission, ©2006 IEEE.)

It should be recognized that using the same oscillator array for both transmit and receive poses a certain complexity. This is true because in the proposed receive array, the oscillator signals are used to *down* convert the signal, so it is the *lower* hybrid frequency of the mixers that is combined to produce the output. Thus the oscillator phases are *subtracted* from the phases of the signals received at the array elements. The result is that the receive phasing of the oscillators is the *conjugate* of the phasing required to transmit a beam in the same direction by using the oscillator signals to excite the elements. If instead the *upper* hybrid frequency were combined on receive, this would not be the case, but the combining for receive would then be done at approximately twice the oscillator frequency rather than at a low intermediate frequency.

In closing this section on receive arrays it should be noted that an array of self-oscillating mixers when properly coupled is synchronized in frequency forming a coupled oscillator array. Coupled self-oscillating mixer (SOM) arrays have been used in retro-directive array applications such as the work by Shiroma et al. [77]. Additionally, the use of coupled SOM arrays in receive phased-array applications has been investigated by Sanagi et al. [78] and ver Hoeye et al. [79]. The array topology proposed in Ref. [78] is shown in Fig. 6-31.

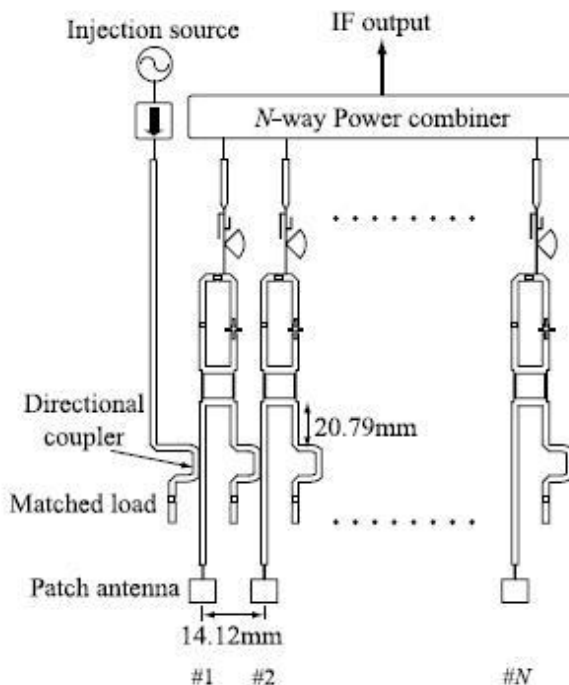


Fig. 6-31. Coupled self-oscillating mixer array.
(Copyright ©2005 IEICE [78].)

The SOM element consists of an amplifier and a branch line coupler providing the necessary feedback to obtain the oscillation. A varactor diode in the feedback loop is used to provide frequency tuning of the individual SOM element. A linear array is considered where the various elements are unilaterally coupled using directional couplers. The RF signal at 17.1 GHz is mixed with the second harmonic of the SOM circuit at 8.5 GHz in order to obtain an IF output at 100 MHz. The SOM array is synchronized to an external injection signal coupled to one of the edge array elements. Sub-harmonic mixing using the second harmonic component results in phase tuning capability of 360 deg. The IF outputs of the SOM array elements are combined using a power combiner. Small prototypes of two and three elements were used to demonstrate the beam-steering capabilities of the proposed architecture. The antenna elements are placed 14.12 millimeters (mm) apart which corresponds to approximately $0.8\lambda_0$ at 17.1 GHz. As a result, the maximum beam scanning angle that can be achieved by this topology is 38.4 deg. Measured radiation patterns of a three element array are shown in Fig. 6-32.

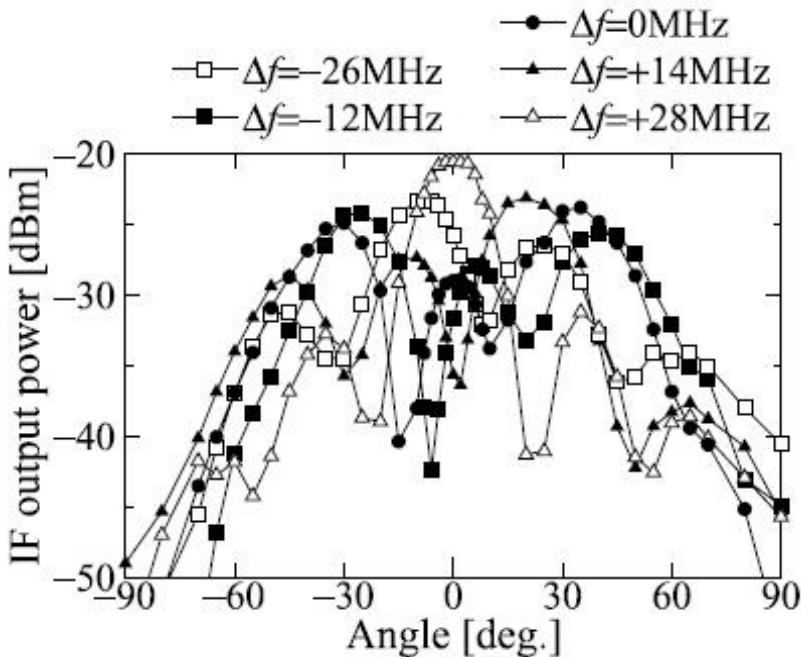


Fig. 6-32. Measured radiation patterns of three-element coupled SOM array. (Copyright ©2005 IEICE [78].)

Radiation patterns were obtained for different (free-running) frequency difference values between the array elements. Variation of the free-running frequency of the synchronized array elements results in variation of the relative phase among the elements. The frequency difference between successive array elements is experimentally mapped to the inter-element phase difference according to Fig. 6-33. As an example, a frequency difference of 28 MHz corresponds to the in-phase state leading to a radiation pattern with a main beam along the broadside direction.

Finally, a four-element receive SOM array was demonstrated by ver Hoeye et al. in Ref. [79]. The circuit topology is shown in Fig. 6-34, followed by the implemented prototype in Fig. 6-35. Each array element is an SOM circuit designed by the authors in [80] and described in Section 8.7. An input RF signal of 11.25 GHz is mixed with the third harmonic of the oscillator at 3.25 GHz, producing an IF output at 1.5 GHz. Using the third harmonic in the mixing product allows for a theoretical phase-tuning range of 540 deg for an individual externally injection locked SOM element. In the proposed circuit topology, an external injection locking signal is applied to all SOM elements using a Wilkinson power-divider network. The SOM elements are not coupled to each other directly; therefore, the array topology can be visualized as a star network where the external injection signal synchronizes all array elements. Each oscillator is connected to a patch antenna and the array outputs are combined using an IF Wilkinson combiner network. A measured beam-scanning range of 23.5 deg was reported.

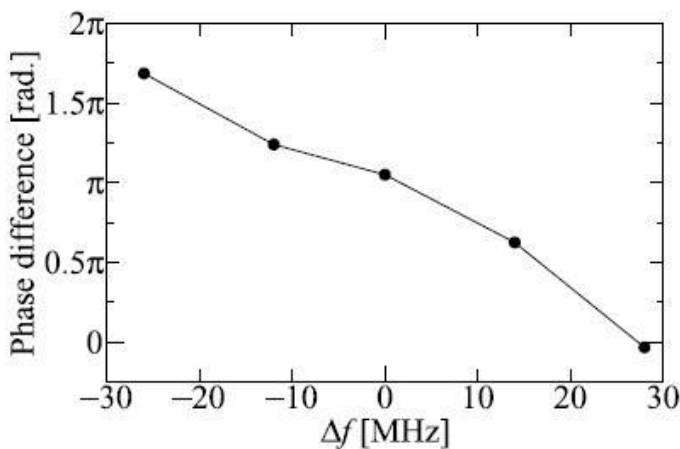


Fig. 6-33. Array element phase difference versus frequency detuning. (Copyright ©2005 IEICE [78].)

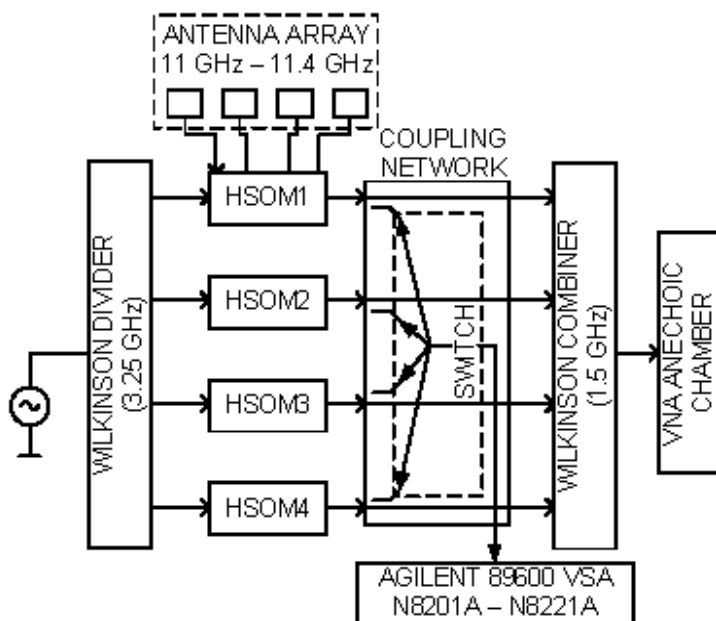


Fig. 6-34. Four-element coupled SOM array block diagram (HSOM = harmonic self-oscillating mixer; VNA = vector network analyzer; VSA = vector signal analyzer). (Adapted from and used with permission [79], ©2009 IEEE.)

6.4 Phase Noise

Throughout the early development of coupled oscillator arrays there was a concern about stability in terms of phase noise. It was recognized that phase control can be enhanced by designing oscillators to have wide locking range because by this means the phase change for a given change in VCO tuning bias is reduced. However, associated with this wider locking range will be lower oscillator Q and an increase in phase noise. Thus, means were sought to mitigate this situation. For example, Chang, et al. were able to double the locking range of a VCO while reducing the phase noise below that expected for such a wide locking range by means of an amplified feedback path [81]. Zheng, et al. reduced the phase noise of an individual oscillator by coupling it to a resonant cavity [82]. Similarly, Colwell and Pearson achieved enhanced locking range via passive feedback [83].

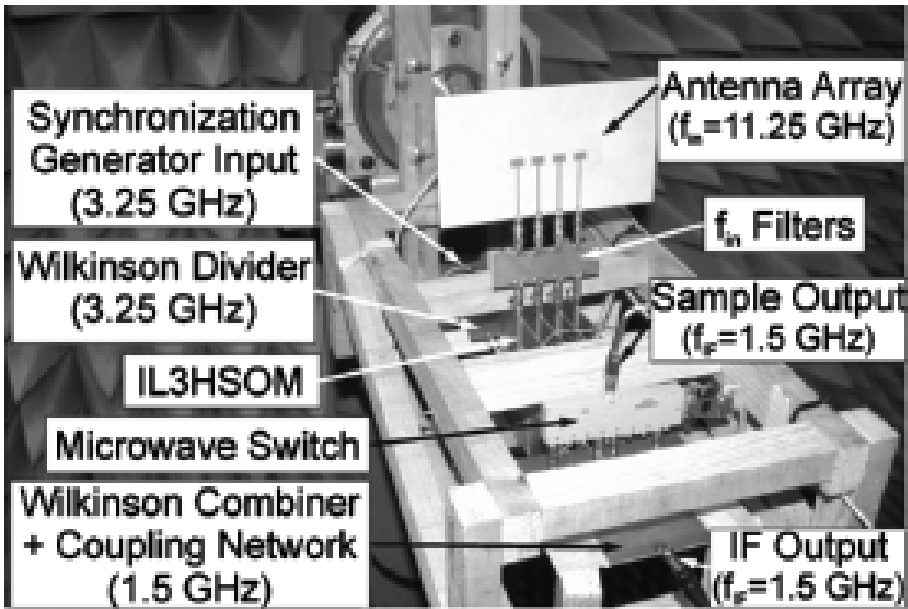


Fig. 6-35. Four-element coupled SOM array implementation. (Reprinted with permission from [79], ©2009 IEEE.)

Aside from the internal design of the oscillators, phase noise is inherently reduced via the coupling and mutual injection locking of a number of oscillators countering the phase noise associated with wide locking range. This phenomenon was studied by Chang, et al. who verified theoretically and experimentally that mutually injection locking N oscillators results in an N -fold reduction in phase noise relative to that of a single one of the oscillators by itself. [84] (See Fig. 6-36.) This happens because the noise signals of the oscillators are incoherent, whereas the carriers are coherent by virtue of the locking. Thus, the carrier voltages add resulting in output power N^2 times that of a single oscillator, whereas the noise powers add resulting in noise power only N times that of a single oscillator. They also showed that the noise increases near the edges of the locking range and reported that no corresponding reduction in phase noise results if the inter-oscillator coupling is unidirectional. An overview of phase noise analysis of coupled-oscillator arrays is presented in Section 7.10.

Recently, a significant decrease in phase noise with increasing coupling strength into the strong coupling regime was reported by Seetharam and Pearson [19]. Interestingly, the behavior of coupled oscillators has been proposed as an alternate means of measuring phase noise rather than the use of a delay line discriminator. [85]

A common method of reducing phase noise is injection locking with a signal from a quiet (stable) external oscillator. As mentioned earlier in Section 6.1, this approach has been investigated in the context of arrays of coupled oscillators by Chang, et al. [59]. They theoretically investigated injection of one or of all of the oscillators and experimented with injection of the center oscillator of a five element array of X-band metal semiconductor field-effect transistor (MESFET) VCOs. They found that near the carrier frequency the noise is reduced to the level of the injection signal, while far from the carrier frequency it reverts to that of the array without external injection. The experimental results are shown in Fig. 6-37.

Dussopt and Laheurte designed a four-element array in a two-by-two configuration using unidirectional coupling to produce circular polarization at 4 GHz. [86] They reported that this configuration produced the expected factor of four reduction in phase noise, but that with unidirectional coupling, this reduction is independent of the coupling phase [87]. Yang, et al. fabricated and tested a similar four-element ring array of linearly polarized elements using bi-directional coupling via lumped capacitors to produce circular polarization at 4.4 GHz [88]. They also experimented with an external injection locking signal.

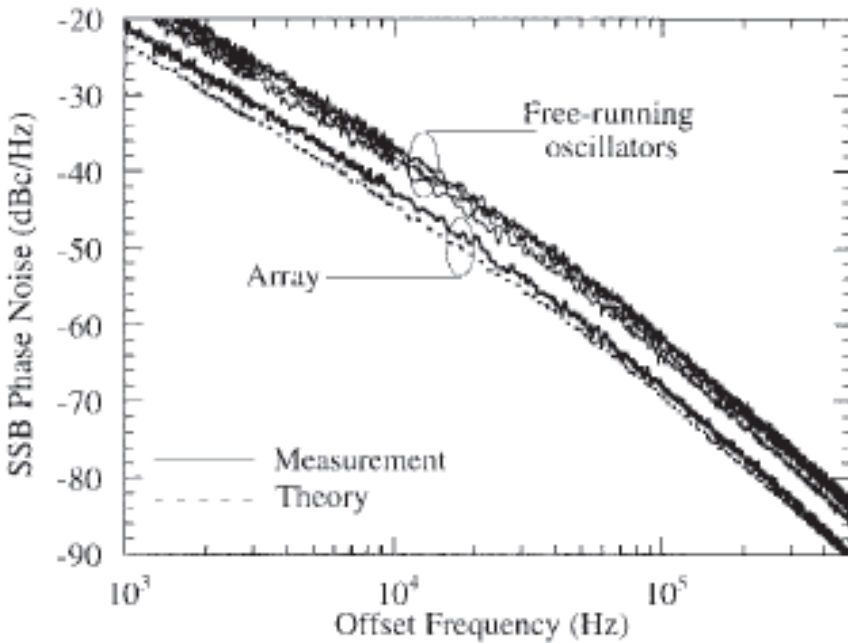


Fig. 6-36. Phase noise of coupled oscillators. (Reprinted with permission from [84], ©1997 IEEE.)

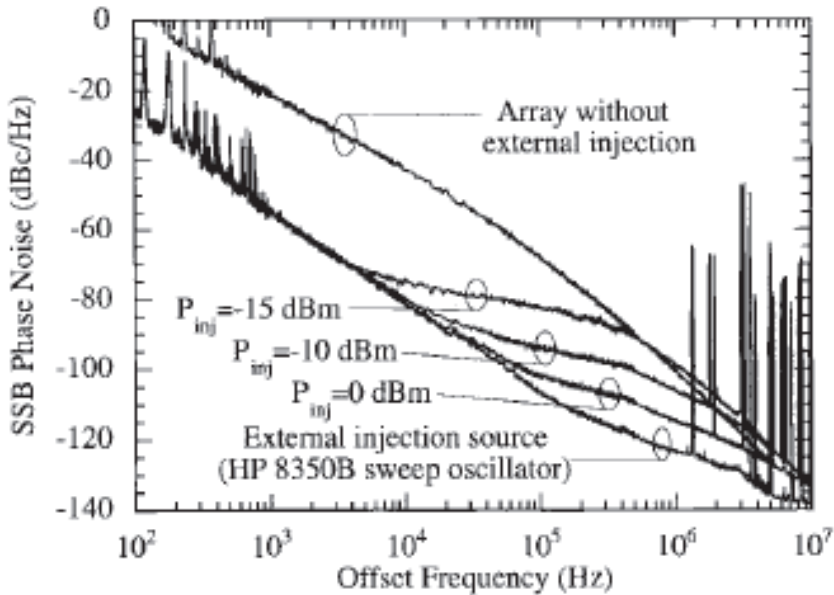


Fig. 6-37. Phase noise of externally injected coupled oscillators. Reprinted with permission from [59]. (©1997 IEEE.)

6.5 The Unlocked State

In the early days of research in microwave coupled oscillators for antenna applications, when spatial power combining was the primary objective, York and Compton observed a phenomenon closely related to mode locking in lasers [5]. The laser cavity supports a large number of modes of oscillation equally spaced in resonant frequency. By modulating a parameter such as the cavity Q at a frequency equal to the mode spacing, these *modes* can be coupled so that the phases of the oscillations become coherent. Under such conditions the sum of the modal signals form a Fourier series, and the laser output becomes a periodic sequence of equal-amplitude pulses. The energy in each pulse is proportional to the square of the number of modes summed because the combining is coherent. York and Compton showed that a similar effect occurs in a coupled oscillator array if the mutually injection-locked state discussed here in connection with beam-steering is *avoided*. In their array, the oscillators were tuned to a set of equally spaced frequencies separated by more than the locking range. Thus, the spectrum of the resulting spatially combined signal consists of a finite number of equally spaced spectral lines, one for each oscillator. The spectral lines are evenly spaced and tend to remain that way. This may be understood on an intuitive level by recalling that the spectrum of an injected but unlocked oscillator has the form shown in Fig. 1-2. In the limit of injection frequency far from the free-running frequency of the oscillator, the line spacing of the

unlocked spectrum is approximately equal to the difference between the injection frequency and the free-running frequency. That is,

$$\sqrt{\Delta\omega_{inj}^2 - \Delta\omega_{lock}^2} \approx \Delta\omega_{inj} \quad (6.5-1)$$

Thus, because the injection signals come from the nearest neighbors, this means that the line spacing of the unlocked spectra is approximately equal to the difference in the free-running frequencies of the neighboring oscillators. In effect then, the oscillators each lock to a line of the unlocked spectrum of their neighbors, and the line spacing of the array becomes uniform. The stability of such mode-locked states has been studied in some detail by Lynch and York [89]. Note that as the differences in the tuning of the neighboring oscillators approach the locking range, the approximation Eq. (6.5-1) fails, the line spacing approaches zero, and the array becomes mutually injection locked, producing a monochromatic output. Maintenance of the mode-locked condition requires that mutual injection locking be avoided. As described in Section 1.4, the locking range can be controlled by adjusting the coupling phase, and in fact, if the coupling phase is 90 deg, the locking range becomes zero, and mutual injection locking is precluded. Thus, from a mode-locking perspective, a 90-deg coupling phase is to be preferred as noted by Lynch and York [89] [90].

One may view the finite line spectrum of the combined output as an infinite line spectrum filtered by a bandpass filter passing only the lines corresponding to the range of oscillator tunings. From Fourier theory, the corresponding time function will be an infinite sequence of equally spaced pulses whose shape is the inverse Fourier transform of the filter bandpass characteristic. For example, if the filter is a square pulse in frequency, the temporal pulses will be sinc functions. York and Compton demonstrated this with an array of three oscillators [5].

A few months later, York and Compton published additional results showing that, when a mode-locked array of oscillators is used to feed a linear array of radiating elements, the resulting beam scans as a function of time [6]. This is a consequence of the fact that the radiating elements are fed with slightly differing frequencies. The frequency differences may be viewed as relative phases changing linearly with time. Thus, the inter-element phasing of the array of elements changes linearly with time, resulting in a beam that scans with time. The repetition rate of the scan is just the period of the pulse output of the array, and at any given angle in the far-zone pattern, the received signal will repeat temporally with this same period as the beam repeatedly scans past that angle.

More recently, the unlocked state of such arrays has been studied as a generator of a chaotic output signal. The array is controlled by modulation of the coupling parameters with the objective of embedding information in the transitioning of the signal between the various unstable periodic orbits [91].

As indicated by York and Itoh [40], all of the phenomena observed for coupled voltage controlled oscillators (VCOs) may also be produced by coupled phase-locked loops (PLLs); one merely has more design flexibility when using PLLs. Section 7.12 contains an introduction to the analysis of coupled phase-locked loops. These principles were demonstrated in a two-element array by Martinez and Compton [92]. This also holds true for mode-locked arrays [93].

6.6 Conclusion

In this chapter we have outlined the experimental work leading to the current level of understanding of the design and fabrication of coupled-oscillator arrays and associated radiating apertures and their performance characteristics. Of course the work has continued as we write, and much of the most recent work severely taxes the capabilities of the linear approximation in explaining the results. Thus, the current trend favors full nonlinear design and analysis. While more complex, such an approach more accurately describes the expected behavior and permits exploitation of the nonlinear effects. These are aspects discussed in Part III of this book.

